Continuation of Fixed-Point Solutions: A Tutorial

Michael Ghil and Andreas Groth

January 10, 2013

Abstract

This tutorial explains the mathematical ideas for the numerical algorithms used in following a branch of equilibrium solutions for a scalar ordinary differential equation (ODE), as well as for an n-dimensional system of ODEs, with respect to changes in a single parameter.

1 Saddle-node bifurcation

The normal form of a (supercritical) saddle-node bifurcation is

$$\dot{x} = \mu - x^2. \tag{1}$$

The stationary solutions of Eq. (1) are given implicitly by

$$f(x;\mu) \equiv \mu - x^2 = 0. \tag{2}$$

These can be written out explicitly, $x = x(\mu)$, as

$$x_\pm = \pm\sqrt{\mu}. \tag{3}$$

To check the stability of either equilibrium in Eq. (3), we add to it a small perturbation Δx, $x = x_\pm + \Delta x$, and substitute this into Eq. (1),

$$\dot{x} = \dot{x_\pm} + \dot{\Delta x} = \tag{4a}$$

$$f(x_\pm + \Delta x) = f(x_\pm) + \left.\frac{\partial f}{\partial x}\right|_{x=x_\pm} \Delta x + O(\Delta x^2). \tag{4b}$$

Since $\dot{x_\pm} = 0 = f(x_\pm)$ and by neglecting higher-order terms in Eq. (4b), we are left with

$$\dot{\Delta x} = \left.\frac{\partial f}{\partial x}\right|_{x=x_\pm} \Delta x. \tag{5}$$

We see that

$$\frac{\partial f}{\partial x} = -2x \begin{cases} < 0 & \text{for } x = x_+ = \sqrt{\mu}\ , \text{ and} \\ > 0 & \text{for } x = x_- = -\sqrt{\mu}. \end{cases} \tag{6}$$

Hence, the upper branch $x_+ = +\sqrt{\mu}$ is stable and the lower branch $x_- = -\sqrt{\mu}$ is unstable.

2 Basics of continuation

Suppose we have found a fixed-point solution,

$$f(x_0;\mu_0) = 0, \tag{7}$$

and we would like to continue this solution in a neighborhood of $(x_0;\mu_0)$. For instance, one can find a stable solution of Eq. (1) by integrating this ODE numerically, forward in time. In fact, this so-called *false-transient* approach to finding a stable fixed point applies to finding solutions of much more complicated systems of n ODEs or even to systems of partial differential equations. Note, however, that it will not work for an unstable fixed point.

In the previous case of the normal form of a saddle-node bifurcation, we already have an explicit equation for $x = x(\mu)$, and it is a simple exercise to find a good approximation of a new solution for a small modification of μ, $\mu = \mu_0 + \Delta\mu$. This can be done with as high a precision as required, as long as we stay away from the bifurcation point itself, where the derivative $\partial f/\partial\mu$ becomes unbounded.

Generally, however, we are only given implicit functions of state variables and parameters, and we look for an explicit solution $x = x(\mu)$ that again fulfills

$$f(x(\mu),\mu) = 0 \tag{8}$$

in a neighborhood of $f(x_0;\mu_0) = 0$. In fact, these functions might only be given numerically at a set of points in the (x,μ)-plane near (x_0,μ_0).

The implicit function theorem guarantees the existence of such an explicit solution. We set the total derivative $\mathrm{d}f$ to be zero,

$$\mathrm{d}f \equiv f_x \mathrm{d}x + f_\mu \mathrm{d}\mu = 0, \tag{9}$$

where $f_x \equiv \partial f/\partial x$ and $f_\mu \equiv \partial f/\partial\mu$ are the partial derivatives, and get

$$\frac{\mathrm{d}x}{\mathrm{d}\mu} = -\frac{f_\mu}{f_x}. \tag{10}$$

This way we are able to update the state variable x with respect to a small modification of the parameter $\mu = \mu_0 + \Delta\mu$, according to

$$x = x(\mu) = x_0 + \left.\frac{\mathrm{d}x}{\mathrm{d}\mu}\right|_{\mu=\mu_0} \Delta\mu + O(\Delta\mu^2) \tag{11a}$$

$$\approx x_0 - \left.\frac{f_\mu}{f_x}\right|_{\mu=\mu_0} \Delta\mu. \tag{11b}$$

Equation (11) is referred to as the *prediction step* in the numerical-continuation algorithm, and it provides a first-order approximation of x in this algorithm. A subsequent corrector of x is necessary to ensure that $f(x,\mu_0+\Delta\mu) = 0$ with sufficiently high accuracy. Such a correction can be obtained by a Newton-type method.

As already indicated in the second paragraph of this section, before Eq. (8), even when using corrections to ensure that one stays on a solution branch, the continuation becomes difficult when approaching a bifurcation point. In the previous example of a saddle-node bifurcation, the partial derivate f_x tends to zero as soon as we approach the bifurcation point, and thus $\mathrm{d}x/\mathrm{d}\mu$ blows up there. To alleviate this difficulty would require an increasingly small step size $\Delta\mu$ as $\mu \to 0$ and one cannot quite reach the turning point nor continue the bifurcation diagram toward the unstable lower branch. Note also that the implicit function theorem does not apply for $f_x = 0$ at the bifurcation point. A mathematical trick to overcome this singularity problem would be to interchange the roles of x and μ, as dependent and independent variable [4], but doing so is impractical for large systems or for several distinct bifurcation points.

3 Pseudo-arclength continuation

A more elegant solution to continuation past bifurcation points is the use of *pseudo-arclength continuation.* The idea is to avoid varying a particular state variable x or parameter μ by parameterizing both via a new variable s,

$$x = x(s), \quad \mu = \mu(s), \tag{12}$$

This way the total derivate becomes

$$\mathrm{d}f = f_x \dot{x}\,\mathrm{d}s + f_\mu \dot{\mu}\,\mathrm{d}s, \tag{13}$$

with $\dot{x} = \mathrm{d}x/\mathrm{d}s$ and $\dot{\mu} = \mathrm{d}\mu/\mathrm{d}s$.

We start as before with an initial fixed-point solution $(x_0; \mu_0)$ such that $f(x_0; \mu_0) = 0$ is satisfied, and try to find a new solution for (x, μ) near $(x_0; \mu_0)$. Since we need to solve for both x and μ in Eq. (12) and we only have one equation to do so, namely $\mathrm{d}f = 0$ in Eq. (13), the system is underdetermined, and so we add the further restriction $\mathrm{d}x^2 + \mathrm{d}\mu^2 = \mathrm{d}s^2$. It is due to this restriction on arclength integration steps that the method is called pseudo-arclength continuation.

With this restriction, we obtain a new, fully determined system for the two-vector $(x, \mu)^{\mathrm{T}}$ as a function of s,

$$\dot{x}^2 + \dot{\mu}^2 = 1, \tag{14a}$$

$$f_x \dot{x} + f_\mu \dot{\mu} = 0. \tag{14b}$$

In this representation, we see that the vanishing of a partial derivate is no longer a problem, and we are finally able to pass the bifurcation point. System (14) can be solved by a predictor-corrector method, where the Newton-type iterations in the corrector are typically restricted to be perpendicular to the branch being continued. This restriction helps, in particular, to pass through turning points of the bifurcation diagram and thus to continue from a stable fixed point — obtained by the method of false transients, say — to the lower branch of a saddle-noddle bifurcation; see, for instance, Fig. B1 in Appendix B of [3].

4 Higher-dimensional systems

Consider next fixed-point continuation in a higher-dimensional system,

$$\mathbf{G}(\mathbf{x};\mu) = 0, \tag{15}$$

with $\mathbf{x} \in \mathbb{R}^n$, $\mu \in \mathbb{R}$, and $\mathbf{G} : \mathbb{R}^n \times \mathbb{R} \to \mathbb{R}^n$. The total derivate now is

$$\mathrm{d}\mathbf{G} = \frac{\partial \mathbf{G}}{\partial \mathbf{x}}\mathrm{d}\mathbf{x} + \frac{\partial \mathbf{G}}{\partial \mu}\mathrm{d}\mu. \tag{16}$$

In the one-dimensional, scalar case of fixed-point continuation with respect to a parameter (Sec. 1), the difficulty at a turning point was that $f_x = 0$. The generalization to $n \geq 2$ is that the Jacobian matrix, $\mathbf{J} \equiv \partial\mathbf{G}/\partial\mathbf{x}$, is going to be singular at a bifurcation point, $\det\mathbf{J} = 0$. In this higher-dimensional case, as stated already at the end of Sec. 2, a simple interchange between a variable and the parameter will no longer help avoid this singularity problem, and so we proceed with pseudo-arclength continuation.

As in the scalar case of Sec. 3, we introduce an arclength variable s and write $\mathbf{x} = \mathbf{x}(s)$ and $\mu = \mu(s)$. Suppose that a particular solution $\mathbf{G}(\mathbf{x}_0;\mu_0) = 0$ is known, e.g. by forward time integration of the system $\dot{\mathbf{x}} = \mathbf{G}(\mathbf{x};\mu)$. We then look in the neighborhood of $(\mathbf{x}_0, \mu_0)$ for a further fixed-point solution $(\mathbf{x}, \mu)$ by integrating

$$\frac{\partial \mathbf{G}}{\partial \mathbf{x}}\dot{\mathbf{x}} + \frac{\partial \mathbf{G}}{\partial \mu}\dot{\mu} = 0, \tag{17a}$$

$$||\dot{\mathbf{x}}||^2 + \dot{\mu}^2 = 1, \tag{17b}$$

where $\dot{\mathbf{x}} = \mathrm{d}\mathbf{x}/\mathrm{d}s$ and $\dot{\mu} = \mathrm{d}\mu/\mathrm{d}s$. Starting from the initial point $(\mathbf{x}_0, \mu_0)$, we are able to continue with a predictor-corrector method, where the Newton-type iterations in the corrector are restricted to a hyperplane perpendicular to the tangent of the continued branch in $\mathbb{R}^n$.

Further details on the continuation of stationary solution branches in general, and on pseudo-arclength continuation and other specific continuation methods with respect to a parameter appear in Appendix B of [3], as well as in [1] and [5]. Once can find more on Newton-type methods — including so-called quasi-Newton methods, in which the functions $f(x;\mu)$ or $\mathbf{G}(\mathbf{x}_0;\mu_0)$ are only given, and hence can only be differentiated, numerically — in Chapter 1 of [2]. All the items in the short bibliography include many further reference sources for the material presented briefly in this tutorial.

References

[1] Doedel, E.; Oldeman, B., Numerical continuation, in *Encyclopedia of Dynamical Systems*, http://www.scholarpedia.org/article/Numerical_continuation

[2] Ghil, M.; Roux, J., *Mathématiques Appliquées aux Sciences de la Vie et de la Planète*, Dunod, Paris, 392 pp.

[3] Legras, B.; Ghil M., Persistent anomalies, blocking and variations in atmospheric predictability, *Journal of the Atmospheric Sciences*, vol. 42 (1985), pp. 433–471.

[4] Roux, J., Définition et caractérisation des points de bifurcation col et fourche, Tutorial from 22 novembre 2012, http://www.environnement.ens.fr/IMG/file/DavidPDF/modelisation/bifurcation_versus_tipping-2.pdf

[5] Simonnet, E.R.; Dijkstra, H.A.; Ghil, M., Bifurcation analysis of ocean, atmosphere and climate models, in *Handbook of Numerical Analysis*, Ed. P.G. Ciarlet, vol. 14 (2009), pp. 187–229.

Here J_T is the truncated Jacobian and Δ_T is the truncated Laplacian of (6).

The kernel of $\mathcal{L}_1$ is composed precisely of all zonal modes (see also Appendix C). Hence (A1) defines uniquely the nonzonal part of ϕ_1, ϕ_1', which does not depend on α, and leaves undetermined the zonal part $\bar{\phi}_1$. The indeterminacy is removed by the solvability condition to second order in $1/\rho$,

$$\int_0^{2\pi}\int_{-1}^{+1} [J_T(\phi_1, \Delta_T\phi_1 + \mu + \mu h) + \alpha\Delta_T\phi_1]Y_l^0 d\mu d\phi = 0, \quad \text{(A2)}$$

which has to be satisfied for all zonal modes Y_l^0 of the truncated solution. The solution thus determined by (A1, A2) is not necessarily the unique solution of (6) in this parameter range, and in fact other solutions exist at large ρ and sufficiently small α which are well separated from Ψ^*.

For ρ tending to 0, we assume $\Psi = \Psi^* + \phi_2$. When α and h are small with respect to unity and of the same order, the nonzonal part ϕ_2' of ϕ_2 is $O(h\Psi^*)$. It is determined to leading order by the balance between the planetary advection and the orographic forcing, which we write for simplicity in continuous form as

$$\frac{\partial\phi_2'}{\partial\lambda} = \mu\frac{\partial\psi^*}{\partial\mu}\frac{\partial h}{\partial\lambda}. \quad \text{(A3)}$$

The zonal part $\bar{\phi}_2$ in this case is $O\left(\frac{h^2}{\alpha}\psi^*\right)$ and determined by

$$-\alpha\Delta_T\bar{\phi}_2 = \overline{J_T\{\phi_2', \mu h\}}, \quad \text{(A4)}$$

where the overbar indicates zonal averaging.

If α is small with respect to h, other solutions, like $\Psi \approx c(\mu + \mu h)$ appear, but the preceding one remains valid. For h still small with respect to 1, but $\alpha \gg h$, (A3) is replaced by the balance between dissipation and orographic forcing,

$$\alpha\Delta\phi_2' = \mu\frac{\partial\psi^*}{\partial\mu}\frac{\partial h}{\partial\lambda}, \quad \text{(A5)}$$

in continuous shorthand. When $\alpha \to \infty$, $\phi_2 = \bar{\phi}_2 + \phi_2' \to 0$, and we recover the statement at the beginning of this Appendix, which holds for finite ρ as well.

The stability of the solutions above depends, in the limit $\rho \to \infty$, on the eigenvalues of the operator $-\Delta_T^{-1}\mathcal{L}_1 - \alpha$, and for $\rho \to 0$ on the eigenvalues of the operator $-\Delta_T^{-1}\mathcal{L}_2 - \alpha$, with

$$\mathcal{L}_2\chi = J_T[\chi, \mu(1 + h)].$$

The eigenvalues of both $\Delta_T^{-1}\mathcal{L}_1$ and $\Delta_T^{-1}\mathcal{L}_2$ are always equal to zero or purely imaginary for $\alpha = 0$ (cf. Appendix C). It follows that, for $\alpha > 0$, all asymptotically valid stationary solutions discussed in this Appendix are stable.

APPENDIX B

Numerical Study of Stationary Solutions

The numerical methods used in integrating the evolution equation (6) were given in LG1, Section 5.1. In this Appendix, we describe therefore only the details of the continuation method (9) used to compute stationary solutions and their stability.

The *pseudo-arclength continuation* method described here is due to Keller (1978) and allows one to follow a solution (Ψ, r) of

$$\mathbf{G}(\Psi, r) = 0, \quad \text{(B1)}$$

where $\mathbf{G}$ is a continuously differentiable map, or C^1-map, from $R^n \times R$ into R^n. We suppose that a particular solution (Ψ_0, r_0) is known and we want to obtain all other solutions (Ψ, r) which are accessible by continuous variation of r. These solutions form a C^1-manifold Γ of dimension 1 in $R^n \times R$, and Γ is parameterized by a curvilinear coordinate s.

Then the problem can be written

$$\mathbf{G}_r\dot{r} + \mathbf{G}_\Psi\cdot\dot{\Psi} = 0, \quad \text{(B2a)}$$

$$\dot{r}^2 + \|\dot{\Psi}\|_2^2 = 1, \quad \text{(B2b)}$$

$$\mathbf{G}(\Psi_0, r_0) = 0, \quad \text{(B3)}$$

where

$$(\dot{\Psi}, \dot{r}) = \left(\frac{d\Psi}{ds}, \frac{dr}{ds}\right).$$

This represents a system of $(n + 1)$ differential equations (B2) for Ψ and r, with initial condition (B3). The essential feature of (B2, B3) is that the nondegenerate singularities of the $n \times n$ matrix $\mathbf{G}_\Psi$ can be treated in this formulation as regular points.

System (B2) is discretized to obtain a series of stationary solutions (Ψ_n, r_n) which approximate the manifold Γ to be explored. The algorithm is divided into two steps. The first step is a first-order forward approximation,

$$\dot{r}_n = \pm[1 + \|\mathbf{G}_\Psi^{-1}(\Psi_n, r_n)\cdot\mathbf{G}_r(\Psi_n, r_n)\|^2]^{-1/2}, \quad \text{(B4a)}$$

$$\dot{\Psi}_n = -\dot{r}_n\mathbf{G}_\Psi^{-1}(\Psi_n, r_n)\cdot\mathbf{G}_r(\Psi_n, r_n), \quad \text{(B4b)}$$

$$\chi_{n,0} = \Psi_n + \sigma\dot{\Psi}_n, \quad \text{(B5a)}$$

$$\xi_{n,0} = r_n + \sigma\dot{r}_n, \quad \text{(B5b)}$$

where σ is a step in curvilinear coordinates. The sign of $\dot{r}_n$ defines the direction of exploration on the manifold Γ; its initial choice is arbitrary. The $\mathbf{G}_\Psi$ above is assumed at first to be nonsingular and $\mathbf{G}_\Psi^{-1}$ is its inverse. We shall see that in practice no difficulty arises from this hypothesis.

The first step, if applied repeatedly by itself, would generate rapidly cumulative errors, and the approximate solution would move away from Γ. This is prevented by the use of a corrector step, which projects the approximation $(\chi_{n,0}, \xi_{n,0})$ back on Γ by using Newton's method to find a solution of (B1).

We solve the problem

$$\mathbf{G}(\Psi_{n+1}, r_{n+1}) = 0, \tag{B6a}$$

$$N(\Psi_{n+1}, r_{n+1}, \sigma) \equiv \dot{\Psi}_n^T \cdot [\Psi_{n+1} - \Psi_n] + \dot{r}_n[r_{n+1} - r_n] - \sigma = 0 \tag{B6b}$$

by a series of iterations of the form

$$\mathbf{G}_\Psi(\chi_{n,i}, \xi_{n,i})\delta\chi_{n,i} + \mathbf{G}_r(\chi_{n,i}, \xi_{n,i})\delta\xi_{n,i} = -\mathbf{G}(\chi_{n,i}, \xi_{n,i}), \tag{B7a}$$

$$\dot{\Psi}_n^T \cdot \delta\chi_{n,i} + \dot{r}_n\delta\xi_{n,i} = -N(\chi_{n,i}, \xi_{n,i}, \sigma), \tag{B7b}$$

$$\chi_{n,i+1} = \chi_{n,i} + \delta\chi_{n,i}, \tag{B8a}$$

$$\xi_{n,i+1} = \xi_{n,i} + \delta\xi_{n,i}. \tag{B8b}$$

The iterations are continued until a convergence criterion is satisfied. The criterion used was that for $i = I$, $\|\mathbf{G}(\chi_{n,I}, \xi_{n,I})\| < \epsilon$, with ϵ prescribed. The new values of (Ψ, r) on Γ are then $\Psi_{n+1} = \chi_{n,I}$ and $r_{n+1} = \xi_{n,I}$.

The constraint (B6b) requires that the projection onto Γ be orthogonal to the direction $(\dot{\Psi}, \dot{r})$. This is a crucial feature of the algorithm, which permits in effect the exploration of Γ to pass through regular turning points of $\mathbf{G}$. Figure B1 illustrates the procedure by comparison with a projection at constant r.

The crossing of a regular turning point must be identified in order to change the sign of $\dot{r}_n$ in (B4a) and to avoid a perpetual movement of the algorithm steps to and fro. This was easy to do in our study since all eigenvalues had to be computed anyway in order to study the stability of the solution. The eigenvalue computation was performed by the QR algorithm as implemented and documented in the International Mathematics and Statistics Library of scientific subroutines (IMSL package).

The required information was thus given by a change of sign of an eigenvalue. More generally, when only the number of eigenvalues with positive real part is needed, Routh's criterion (Guillemin, 1949) may be applied to see whether this number changes by one, as it does at a turning point, or by two, as it does at a Hopf bifurcation point.

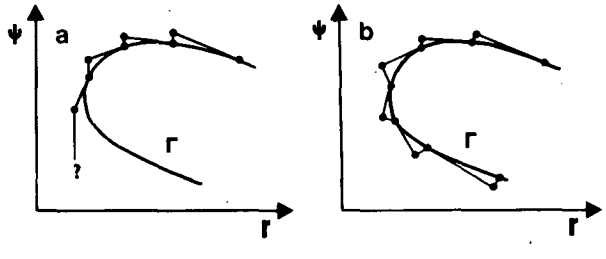

FIG. B1. Successive iterations of a continuation method (B4, 5). (a) With parallel projection only, leading to divergence of the algorithm at a turning point; (b) with a Newton correction (B6–8), equivalent to perpendicular projection from the prediction onto the solution branch.

The value of the step length σ determines the performance of the algorithm. Too small a value needlessly increases the computation time, whereas too large a value may cause divergence or a jump from one branch of solutions to another. Keller (1978) gives an estimate of σ that depends on second derivatives of $\mathbf{G}$.

We have used a single value of σ, fixed for each exploration. A set of values, suitable for all situations, has been established by trial and error. Among other possible strategies, Li and Yorke (1980) propose to control the angle between two consecutive tangent vectors on Γ limiting it to an empirically predetermined maximum and reducing σ if the limit is exceeded during one arclength step. This procedure allows simultaneous control of the crossing of regular turning points.

The application of the algorithm implies the nonsingularity of $\mathbf{G}_\Psi$, which seems to contradict the crossing of turning points. But if the turning point is nondegenerate, the probability is very small that an iteration of the algorithm fall sufficiently close to the turning point for $\mathbf{G}_\Psi$ to be numerically singular. Should this occur nonetheless, a slight modification of σ suffices, in practice, to eliminate the singularity.

It may be advantageous in order to improve the conditioning of Newton's method (B7) to replace the L_2 norm by another one in the condition (B2b). We have used in fact for the cross sections in ρ:

$$\dot{\rho}^2 + a\nabla_T\dot{\Psi} \cdot \nabla_T\dot{\Psi} = 1, \tag{B9}$$

with $a = 10$ and ∇_T the spatial gradient of the truncated field $\dot{\Psi}$. This induces a straightforward modification of the other steps, where the old norm is replaced by the new one. With this new norm, the curvature of Γ is smoother than with the L_2 norm and larger values of σ can be used.

Several variations and improvements on the method have been proposed. Li and Yorke (1980) replace the first-order forward predictor step by an explicit Runge-Kutta scheme. Glowinski (1984) replaces Newton's method by a conjugate-gradient algorithm. Kubiček and Marek (1983, p. 39) do not correct the predictor step by an orthogonal projection, but keep fixed one component of the state vector Ψ chosen by a maximum pivoting criterion.

From the point of view of further applications of this method to meteorological problems, it is important to realize that the method is in extensive routine use for the solution of nonlinear partial differential equations depending on one or more parameters in fluid dynamics, elasticity and other areas of continuum physics. Studying the stability of stationary solutions and nonlinear resonance for spatially two- and three-dimensional models of large-scale atmospheric dynamics is thus entirely feasible on currently available computers or on those expected within a decade.

It is also noteworthy from this point of view that exact Newton iteration in (B7) can be replaced by quasi-Newton (QN) iteration, i.e., the Jacobian matrices of partial derivatives $\mathbf{G}_\Psi$ and $\mathbf{G}_r$ can be replaced by partial difference matrices (Dennis and Moré, 1977; Kubiček and Marek, 1983, p. 51). The latter are much easier to program for large, three-dimensional atmospheric models such as general circulation models.

APPENDIX C

Linear Resonances for Small Topography

In the limit of vanishing topographic amplitude, $h_0 = 0$, Ψ^* is a stationary solution of (6) for all values of ρ and α. When h_0 is small enough, a perturbed solution $\Psi = \Psi^* + \phi_3$ obtains, with ϕ_3 satisfying to first order in h_0 and $\alpha = O(h_0)$

$$\mathcal{L}_3\phi_3 \equiv \rho J_T(\Psi^*, \Delta_T\phi_3) + \rho J_T(\phi_3, \Delta_T\Psi^*) + J_T(\phi_3, \mu) = -J_T(\Psi^*, \mu h). \quad \text{(C1)}$$

Equation (C1) defines the nonzonal part of ϕ_3. All zonal modes are in the nullspace of $\mathcal{L}_3$. This part of the kernel does not induce a singularity in general since the right-hand side does not possess a zonal part. However, such singularities may occur for special values of ρ, for which $\mathcal{L}_3$ also possesses a nonzonal null vector. Therefore in this Appendix we derive the solution of the zero eigenvalue problem for $\mathcal{L}_3$, concentrating on the modes with zonal wavenumber $m = 2$, which contain the orography and the right-hand side of (C1).

From the definition (5b), we have $\psi^* = -\kappa\mu^3$ with $\kappa = 0.2598$. Two useful relations are then

$$\Delta\mu^3 = 6\mu(1 - 2\mu^2) \quad \text{(C2)}$$

and the three-term recursion property (see also Balgovind *et al.*, 1983)

$$\mu^2 P_l^m(\mu) = a_l^m P_l^m(\mu) + b_l^m P_{l+2}^m(\mu) + c_l^m P_{l-2}^m(\mu), \quad \text{(C3a)}$$

with

$$a_l^m = \frac{2l^2 - 2m^2 + 2l - 1}{(2l - 1)(2l + 3)}, \quad \text{(C3b)}$$

$$b_l^m = \frac{(2l + 1)^{1/2}}{(2l + 5)^{1/2}} \frac{[(l + 1)^2 - m^2]^{1/2}[(l + 2)^2 - m^2]^{1/2}}{4(l + 1)^2 - 1}, \quad \text{(C3c)}$$

$$c_l^m = b_{l-2}^m. \quad \text{(C3d)}$$

With (C2) and (C3), one obtains

$$\mathcal{L}_3 Y_l^m = \mathrm{i}m\kappa\rho[(X + \tilde{a}_l^m)Y_l^m + \tilde{b}_l^m Y_{l+2}^m + \tilde{c}_l^m Y_{l-2}^m], \quad \text{(C4a)}$$

using the auxiliary variables $X = (1 - 6\kappa\rho)/\kappa\rho$, $d_l = 36 - 3l(l + 1)$ and

$$\{\tilde{a}_l^m, \tilde{b}_l^m, \tilde{c}_l^m\} = d_l\{a_l^m, b_l^m, c_l^m\}. \quad \text{(C4b)}$$

For a given zonal wavenumber m, the matrix A of $-i\mathcal{L}_3/m\rho\kappa$ is tridiagonal, since only odd values of l are present, and has real coefficients. The resonances of $\mathcal{L}_3$ are given by the values of X which cancel the determinant of A. Moreover, A is of the form $\mathsf{A} = XI - \tilde{\mathsf{A}}$; the problem thus reduces to finding the eigenvalues X of a tridiagonal real matrix $\tilde{\mathsf{A}}$.

Since the entries of $\tilde{\mathsf{A}}$ are nonnegative, the largest eigenvalue in absolute value is necessarily real and positive. Moreover, $\tilde{\mathsf{A}}$ is diagonally dominant,

$$|\tilde{a}_l^m| \geq |\tilde{b}_l^m| + |\tilde{c}_l^m|,$$

so that its eigenvalues have the same sign as those of its diagonal entries, $-\tilde{a}_l^m$, i.e., nonnegative.

For $m = 2$ and the truncation scheme shown in Fig. 1, we have

$$-\tilde{\mathsf{A}} = \begin{bmatrix} \tilde{a}_3^2 & \tilde{b}_3^2 & 0 & 0 \\ \tilde{c}_5^2 & \tilde{a}_5^2 & \tilde{b}_5^2 & 0 \\ 0 & \tilde{c}_7^2 & \tilde{a}_7^2 & \tilde{b}_7^2 \\ 0 & 0 & \tilde{c}_9^2 & \tilde{a}_9^2 \end{bmatrix}. \quad \text{(C5)}$$

Since $\tilde{a}_3^2 = \tilde{b}_3^2 = \tilde{c}_5^2 = 0$, $X_0 = 0$ is an eigenvalue of $\tilde{\mathsf{A}}$. The three other solutions of the characteristic equation for $\tilde{\mathsf{A}}$ are $X_1 = 12.08$, $X_2 = 48.75$ and $X_3 = 136.3$, so that all eigenvalues are indeed real and nonnegative.

These values of X lead respectively to the linearly resonant parameter values $\rho_0^R \approx 0.6145$, $\rho_1^R \approx 0.2129$, $\rho_2^R \approx 0.07030$ and $\rho_3^R \approx 0.02705$, which are indicated on the abscissa in Fig. 4. They initiate clearly the nonlinear resonances apparent in the figure at finite values of h_0.

As a by-product of this analysis, we can also derive properties of the operator $\Delta_T^{-1}\mathcal{L}_1$ defined in Appendix A, since $\mathcal{L}_1$ and $\mathcal{L}_3$ differ only by a diagonal term. Each m-block of the matrix $-\Delta_T^{-1}\mathcal{L}_1$ has the same structure as that of $-i\mathcal{L}_3/m\kappa\rho$.

From this we deduce immediately that all eigenvalues of $\Delta_T^{-1}\mathcal{L}_1$ corresponding to zonal modes are zero, while they are purely imaginary and nonzero for nonzonal modes. For $m = 2$, the eigenvalues are respectively $\sigma_0 = \pm 12i$, $\sigma_1 = \pm 36.6i$, $\sigma_2 = \pm 109.5i$ and $\sigma_3 = \pm 284.6i$, conjugate values appearing when one considers $\mathcal{L}_1 Y_l^m$ and $\mathcal{L}_1 Y_l^{-m}$.

The results above allow us to explore the behavior of resonances when one extends the truncation in total wavenumber l at a given zonal wavenumber m. We preserve here the same symmetries as in the basic truncation scheme and thus consider only odd values of l.

Let A_L be the matrix associated with the truncation at $l = L$. We have the following recursion relation for its determinant D_L:

$$D_L = (\tilde{a}_L^m + X)D_{L-2} - \tilde{b}_L^m \tilde{c}_L^m D_{L-4}.$$

It is more convenient at this point to return to the matrix A'_L with entries (C3b–d), yielding the recursion